Cardiac Arrhythmias Induced by an Electrical Stimulation at a Cellular Level

S Jacquir[1], S Binczak[1], D Vandroux[2],
G Laurent[3], P Athias[2], JM Bilbault[1]

[1]Laboratory LE2I UMR CNRS 5158, University of Burgundy, Dijon, France
[2]Institute of Cardiovascular Research, University Hospital Center, Dijon, France
[3]Cardiology Department, University Hospital Center, Dijon, France

Abstract

To provide insights into the impulse propagation between cardiac myocytes, we performed studies of excitation spread with cellular resolution in confluent monolayers of cultured cardiomyocytes (CM). Multisite field potentials have been recorded using microelectrode arrays (MEA) technology in a basal condition and in proarrhythmic conditions induced by a high frequency electrical stimulation. The in vitro observation of spiral waves opens a new way to test the anti-arrhythmic drugs or strategies at cellular level.

1. Introduction

Among the reentrant arrhythmias, our study focused on the fibrillation phenomenon, which is characterized by a high irregular excitation rate responsible for erratic atrial contractions (e.g. atrial fibrillation). The reentrant phenomenon is described as a wavefront that reenters and hence re-excites the same area repeatedly as opposed to the normal 'planar' wavefront generated by the sinus node that depolarizes the myocardial tissue only once per cardiac cycle. During a fast fibrillatory rhythm, re-excitations occur at a rate higher than the normal sinus rhythm, which in turn is overdriven. Experimental evidence that functional reentrant spiral waves (SW) are present in rabbit cardiac atrial was first given by [1], and later on by [2, 3] and [4]. The idea that atrial or ventricular fibrillations are both caused by multiple chaotically wandering electrical wavelets, leading to chaotic uncoordinated contractions, was first formulated by [5]. However, opinions differ on how these wavelets arise. According to the spiral breakup hypothesis, wavelets are the result of the fragmentation of an initial "mother" spiral wave [6, 7]. According to the fibrillatory conduction hypothesis, wavelets are the result of a single excitation source [8, 9, 10]. This source emits waves at such a high frequency that, because of tissue heterogeneities, they cannot be conducted at a 1 to 1 ratio in all parts of the tissue. The aim of our investigation was to induce an experimental fibrillation phenomenon in order to identify, at a cellular level, the electrophysiological mechanism involved in its initiation and perpetuation. At First, we have studied spontaneous electrical activities of cultured neonatal rat cardiomyocytes using a Micro-Electrode Array (MEA) system. Field potentials (FP) corresponding to the extra-cellular potentials from a 2-4 cells area were recorded to approximate activation maps with one "electrical unit" resolution. Therefater, cardiomyocytes have been submitted to a high frequency burst stimulation, which was applied at the edge of the MEA. This high rate stimulation was able to induce fast and irregular electrical activities which mimicked fibrillation patterns. These fibrillation waves were analyzed more precisely by reconstructing the electrical activation maps. The section (2) describes materials and methods. The section (3) presents some preliminary results and the last section (3) concludes and gives perspectives of our works.

2. Materials and methods

2.1. Cardiomyocyte culture preparation

Neonatal ventricular myocytes were prepared from 1 to 4 days-old Wistar rats by trypsin-based enzymatic dispersion as described previously [11]. The cell suspension was preplated twice in in the culture medium composed of Ham's $F10$ medium supplemented with fetal calf serum (FCS) and penicillin/streptomycin (100 U/ml) in order to increase cardiomyocyte proportion. Cardiomyocyte-rich cultures ($> 90\%$) were seeded at a final density of 10^5 cells per cm^2 in the cultured medium. Cultures were incubated in a humidified incubator (95% air, 5% CO_2 at 37° C) and were used after 4-5 days of growth, a step at which confluent and spontaneously beating cell monolayers were obtained.

2.2. Multielectrode array recordings

CM were grown on multielectrode arrays (MEA) allowing non-invasive synchronous multifocal field potential (FP) recordings. The MEA consists of 60 substrate-

integrated microelectrode arrays (8×8 matrix, 30 μm electrode diameter, 200 μm inter-electrode distance). Data were acquired and analyzed with a customized platform programmed with Matlab (Mathworks) in order to provide two-dimensional electrophysiological maps derived from these multisite FP recordings.

3. Results

In a first time, the FP propagations in the physiological conditions were investigated. Recorded data have been classified between the normal and the artefactual signals (see Fig.1). This classification process includes differ-

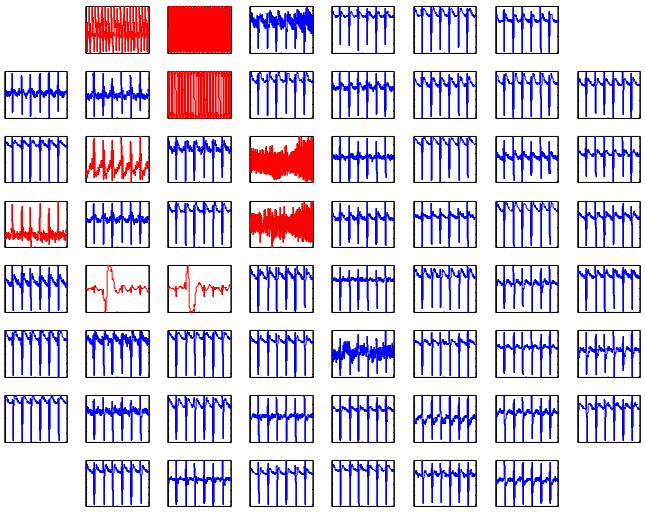

Figure 1. Field potential signals. Each panel corresponds to a single electrode. Correct signals are in blue and artefactual signals are in red.

ent steps. In first step, a FP time serie is binarized using a suitable threshold α defined by

$$\alpha_i = m_{S_i} + \left| \frac{\overline{S_i} - m_{S_i}}{2} \right| \quad (1)$$

with $i = 1$ to 60 is a number of electrodes, m_{S_i} is a minimum value of the FP peak corresponding to a train of FP spikes S and $\overline{S_i}$ is a mean value of the FP train.
After this binarization step, for each train of the FP, a classification parameter β is calculated

$$\beta_i = \overline{P_{Sb_i}} - \frac{\sigma_{P_{Sb_i}}}{2} \quad (2)$$

where $\overline{P_{Sb_i}}$ is the mean of the periods corresponding to the binarized signal Sb of the electrode i and σ is the standard deviation of the period. So, the classification is given by these two conditions :

- If $\overline{P_{Sb_i}} > \beta_i$ then the FP spikes were considered as the normal signal (blue signal in the Fig. 1);

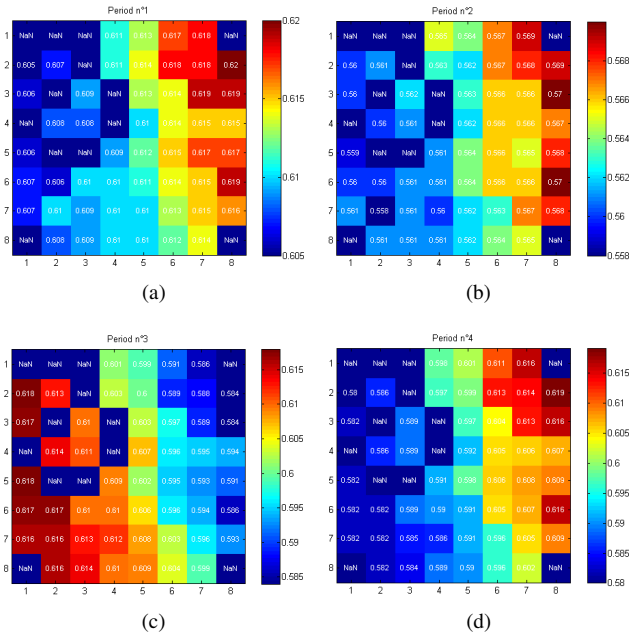

Figure 2. First four periods of the field potential. Panel (a) is the first period and panel (d) is the fourth period.

- If $\overline{P_{Sb_i}} < \beta_i$ then the FP spikes were classified as artefactual signal (red signal in the Fig. 1).

Figure 1 illustrates the classification result. Then, the variability of the FP frequency was analyzed. Figure 2 presents the distribution of the first four periods of the FP train corresponding to data presented in Fig. 1. This analysis indicates the sligth variability of the FP frequency. This variability may be due to a remodelling phenomenon of gap junctions [12], or the fluctuation of the ionic channels or changes in the propagation path. This last hypothesis appeared consistent with previous propagation data from intracellular recordings of the action potentials [13, 14]. After determining the local activation time (LAT) of each FP spike, the activation map enables to quantify the propagation path of the FP spikes during each period. The activation maps corresponding to the signals in Fig. 1 are reported in the figure 3. The number inserted in each colored patch corresponds to the rank of the FP spike activation (refer to Fig. 3a). From a global view of activation maps, we can conclude that the FP spike propagates following a linear path (see white arrow in the Fig. 3). However, the examination of the individual rank of order of FP spike activation revealed that the FP spike propagation pathway fluctuated at each period. This might mean that the FP cell to cell propagation was nonlinear, although the overall propagation throughout the multicellular sheet was linear.

After studying the FP propagation in physiological conditions, cardiomyocytes were stimulated by an external electrical signal, consisting in a stimulation train (burst of 200 μV at 100 Hz during 5 min) in one point at the edge of the

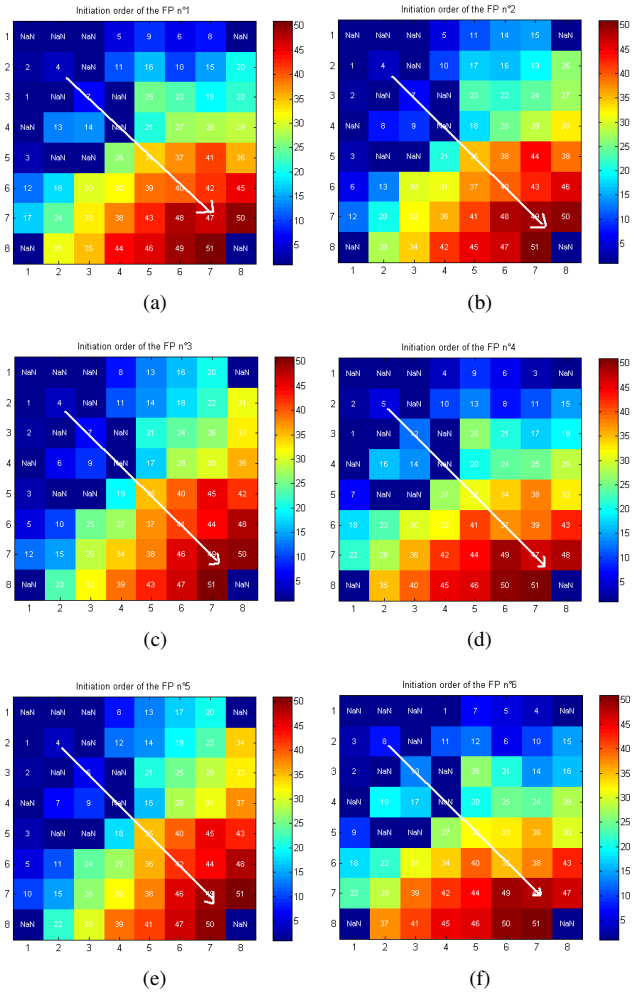

Figure 3. The local activation maps of the Field potential. Panel (a) is the first map and panel (f) is the sixth map.

MEA. After this stimulation protocol, the recorded electrical activities were fast and irregular as illustrated in Fig. 4. The rate was irregular as compared to control cells (Fig. 1). This change was confirmed by Poincaré maps of the FP periods. In the case of control cells (Fig. 1), stable fixed points are found in a Poincaré map for each individual electrode. Points (cross in Fig. 5) can be considered like attractors. They are situated along a bissector (continuous line in Fig. 5). In this case, the FP frequency was regular and stable in a period of time. In the case of stimulated cells, the number of attractors is different for each electrode. Attractors are not stable and move around the bissector (see Fig. 6).
Activation mapping during a regular rhythm revealed a planar propagation wavefront (see Fig. 3). The observation of activation map during arrhythmias revealed an average of 3 ± 1 SW within the surface mapped. Rotation waves appeared to be random and could change from one period to another. SW were unstable in location and could move

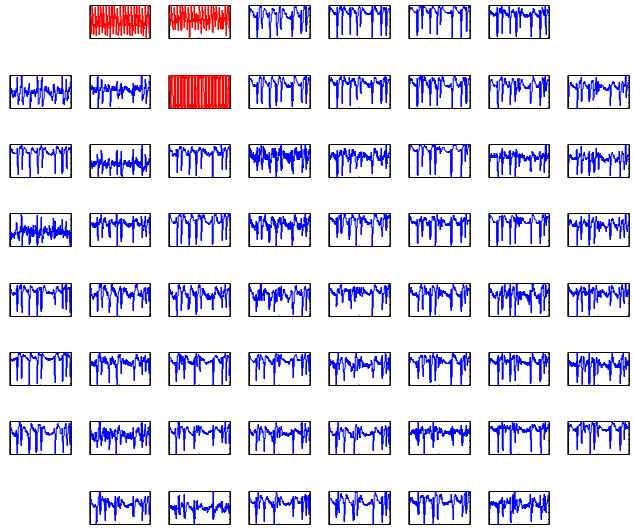

Figure 4. Field potential signals. Each signal corresponds to one electrode. Conform signal is in blue color and non conform signal is in red color.

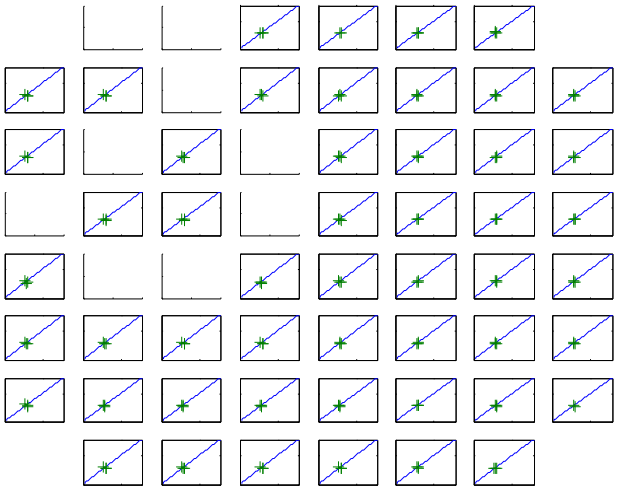

Figure 5. Poincaré maps of field potential periods corresponding to control cells (signals in Fig. 1).

inside or outside the recording area. SW had a mean radius of 400 $\pm$ 100 μm and a mean angular velocity of 225 $\pm$ 30 rotations per minute. Unstable reentrant and colliding wavefronts were also observed during a total of 180 min per arrhythmic episode.

4. Discussion and conclusions

In this work, cardiac impulse propagation has been investigated and sustained fast irregular arrhythmia have been induced in neonatal rat cultured CM. According to the results presented here, unstable spiral waves with randomly changing location and rotation waves can be precisely character-

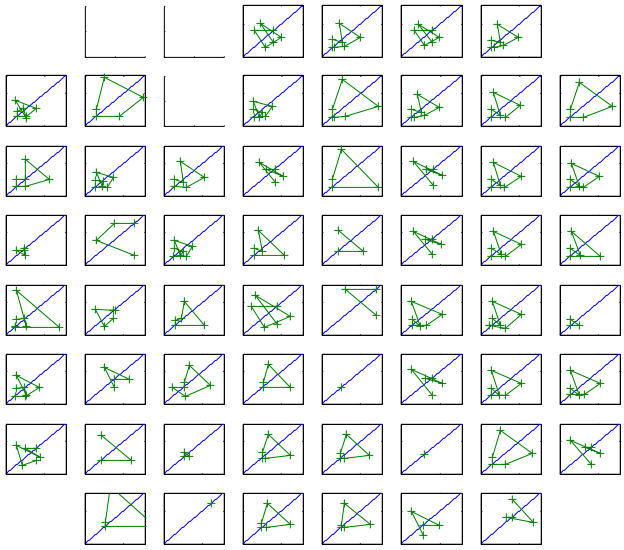

Figure 6. Poincaré maps of field potential periods corresponding to cells submitted to field stimulation (signals in Fig. 4).

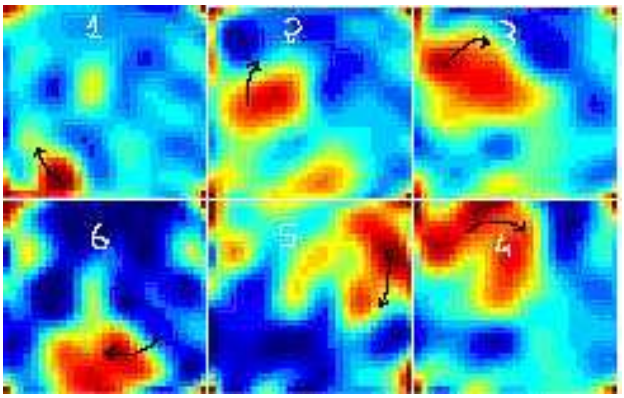

Figure 7. Series of snapshots displaying a relatively stable counter-rotating spiral wave during a sustained induced arrhythmia episode (the arrows indicate the clockwise rotation). Experimental data were smoothed using a cubic spline interpolation. The panel 1 shows the initiation of the SW and the last panel (6) illustrates the termination of the SW. The black color indicates the depolarization of cells and the white color indicates the refractory period.

ized using a MEA data acquisition system. This novel in vitro model of sustained induced arrhythmias, mimicking fibrillation patterns, may be helpful in the comprehension of atrial fibrillation in clinical situations and be useful for testing AF interventions. Whithin the limitations inherent to the preparation used, the cultured CM monolayer is a controlled experimental model that may be useful for further studies on the basic aspects of fibrillation and defibrillation.

References

[1] Allessie MA, Bonke FIM, Schopman FJG. Circus movement in rabbit atrial muscle as a mechanism of tachycardia. Circ. Res. 1973; 33: 54-62.

[2] Davidenko JM, kent PF, Chialvo DR, Michaels DC and Jalife J, Sustained vortex-like waves in normal isolated ventricular muscle. Proc. Natl. Acad. Sci. U.S.A. 1990; 87: 8785-8789.

[3] Davidenko JM, Pertsov AM, Salomonsz R, Baxter W and Jalife J, Stationary and drifting spiral waves of excitation in isolated cardiac muscle. Nature. 1992; 335: 349-351.

[4] Pertsov AM, Davidenko JM, Salomonsz R, Baxter W and Jalife J, Spiral waves of excitation underlie reentrant activity in isolated cardiac muscle. Circ. Res. 1993; 72: 631-650.

[5] Moe GK, Rheinboldt WC and Abildskov JA, A computer model of atrial fibrillation. Am. Heart. J. 1964; 67: 200-220.

[6] Panfilov AV and Pertsov AM, Ventricular fibrillation: evolution of the multiple wavelet hypothesis. Phil. Trans. R. Soc. Lond. 2001; A 359: 1315-1325.

[7] Weiss JN, Chen P, Qu Z, Karagueuzian HS, Lin S and Garfinkel A, Electrical restitution and cardiac fibrillation. J. Cardiovasc. Electrophysiol. 1964; 13: 292-295.

[8] Jalife J, Gray R, Morley GE and Davidenko JM, Self-organization and the dynamical nature of ventricular fibrillation. Chaos. 1998; 8: 7993.

[9] Jalife J, Ventricular fibrillation: mechanisms of initiation and maintenance. Annu. Rev. Physiol. 2000; 62: 2550.

[10] Zaitsev AV, Berenfeld O, Mironov SF, Jalife J and Pertsov AM, Distribution of excitation frequencies on the epicardial and endocardial surfaces of fibrillating ventricular wall of the sheep heart. Circ. Res. 2000; 86: 408417.

[11] Grynberg A. Primary rat cardiac cell culture: diet of the mother rats as a determinant parameter of cardiomyoblast production from neonates. Biol. Cell 1986; 57: 89-92.

[12] Rohr S. Role of gap junctions in the propagation of the cardiac action potential. Cardiovasc Res 2004; 62: 309-322.

[13] Jacquir S, Laurent G, Tissier C, Vandroux D, Devillard L, Brochot A, Rochette L, Binczak S, Wolf JE, Bilbault JM, Athias P. Simultaneous paired intracellular microelectrode study of the impulse propagation in cardiomyocyte culture. Archives des Maladies du Coeur et des Vaisseaux. 2005; 98(4): 392.

[14] Jacquir S, Binczak S, Rosse M, Vandroux D, Laurent G, Athias P, Bilbault JM. Multisite Field Potential Recordings and Analysis of the Impulse Propagation Pattern in Cardiac Cells Culture. IEEE Computers in Cardiology Proceedings. 2007; 34: 125-128.

Address for correspondence:

Dr Sabir Jacquir
Laboratory of electronics, computer science and image (LE2i), University of Burgundy, 9 avenue Alain Savary, BP 47870, 21078 Dijon, France,
sjacquir@u-bourgogne.fr